

## Electronic Supplementary Information

### Facile fabrication of graphene-polypyrrole-Mn composites as high performance electrodes for capacitive deionization

Xiaoyu Gu, Yu Yang, Yang Hu, Meng Hu, Jian Huang and Chaoyang Wang\*

**Table S1** – BET results of samples.

Samples	Specific surface area (m <sup>2</sup> /g)	Average pore diameter (nm)	Total pore volume (cm <sup>3</sup> /g)
RGO	120	8.6	0.31
PPy	63	10.8	0.21
RGO-PPy <sub>0.5</sub> -Mn <sub>0.4</sub>	331	8.6	1.07
RGO-PPy <sub>0.5</sub> -Cu <sub>1</sub>	144	8.8	0.33

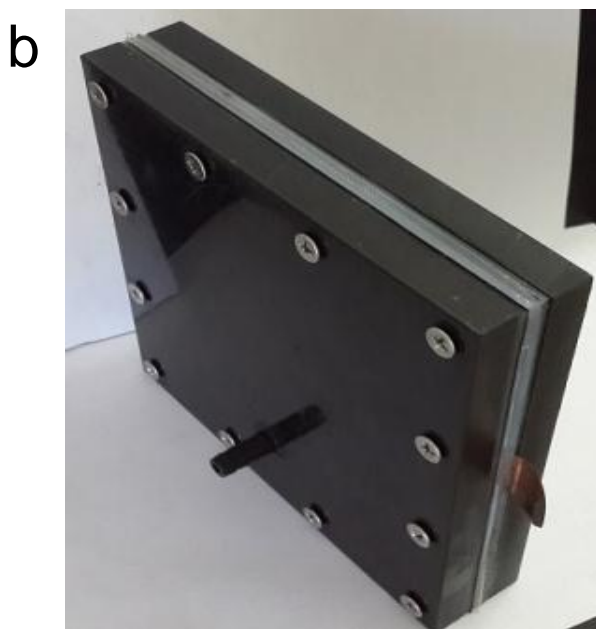
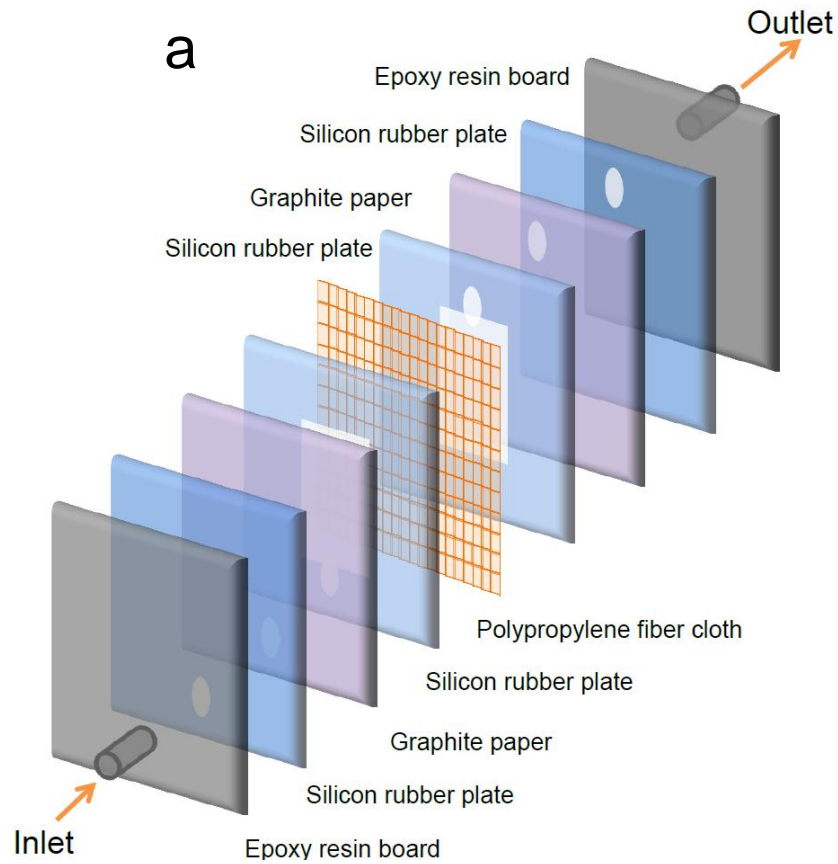


**Fig. S1** - (a) Schematic illustration of single CDI device and (b) photo of the combined CDI device.

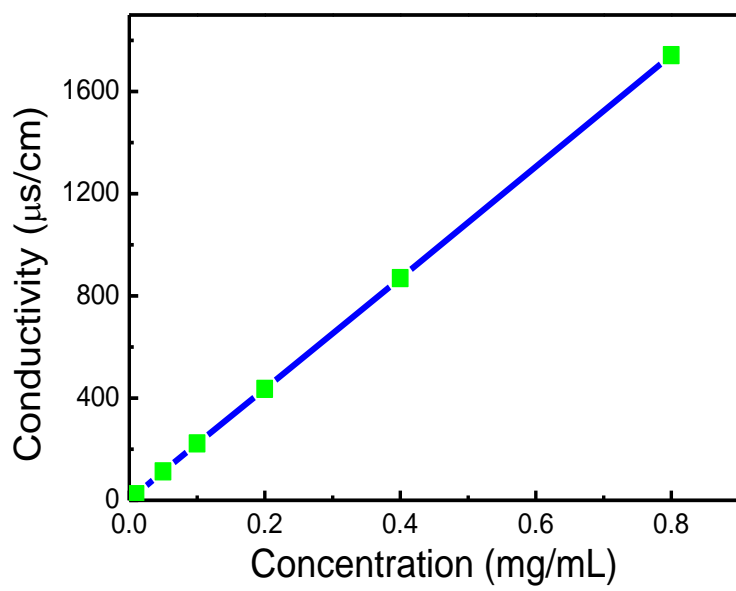


**Fig. S2** - Relationship between conductivity and concentration of NaCl solutions.

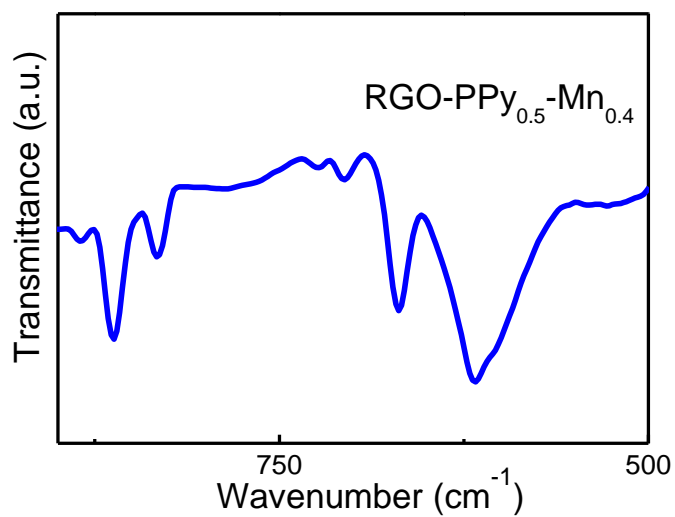


**Fig. S3** - FT-IR spectra of RGO-PPy-Mn composites from 900 to 500  $\text{cm}^{-1}$

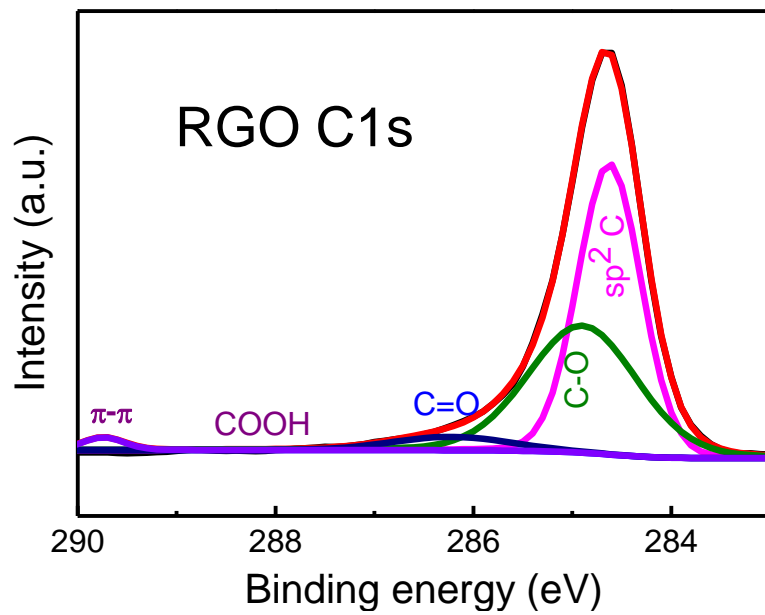


**Fig. S4** - XPS C1s spectra of RGO.

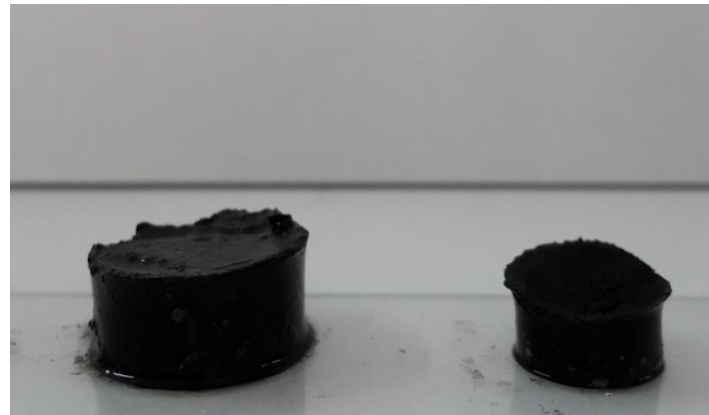


**Fig. S5** - Photo of RGO-PPy and RGO hydrogels.

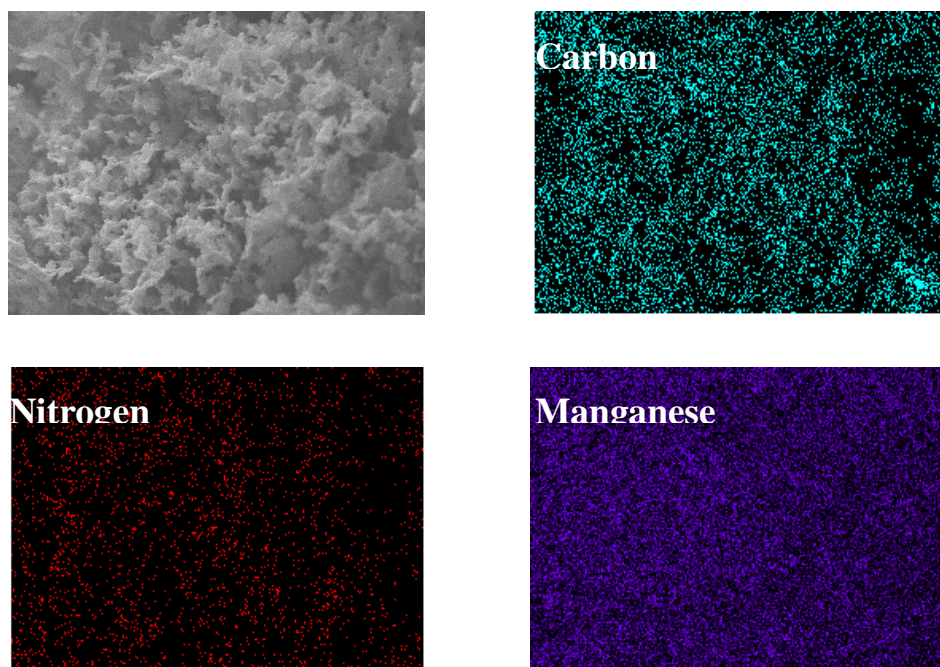


**Fig. S6** - SEM image and C-, N- and Mn- elemental mappings for RGO-PPy-Mn composites.

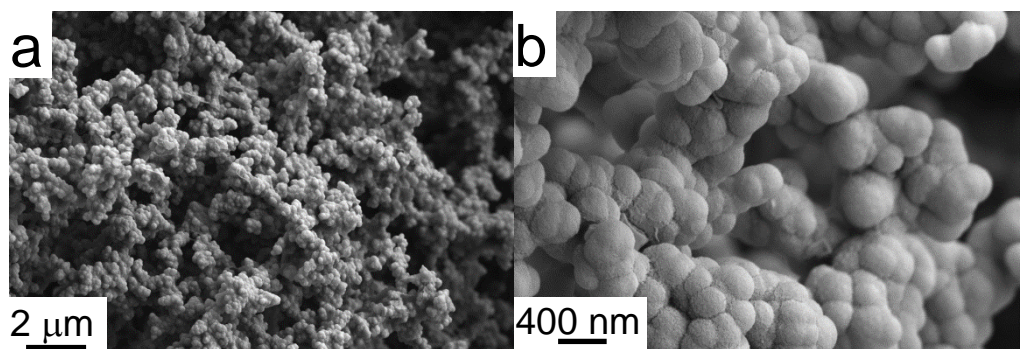


**Fig. S7** - (a,b) SEM images of PPy nanoparticles with different magnifications.

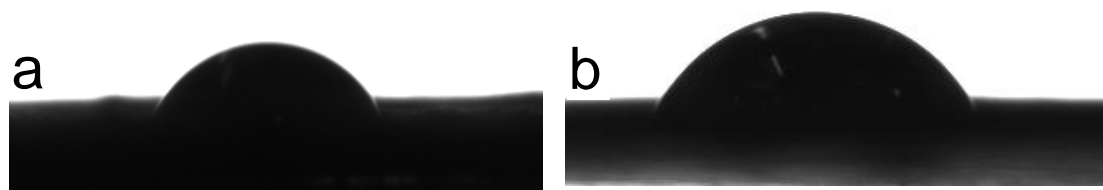


**Fig. S8** - Contact angle images of water droplets on (a) RGO and (b) RGO-PPy-Mn electrodes

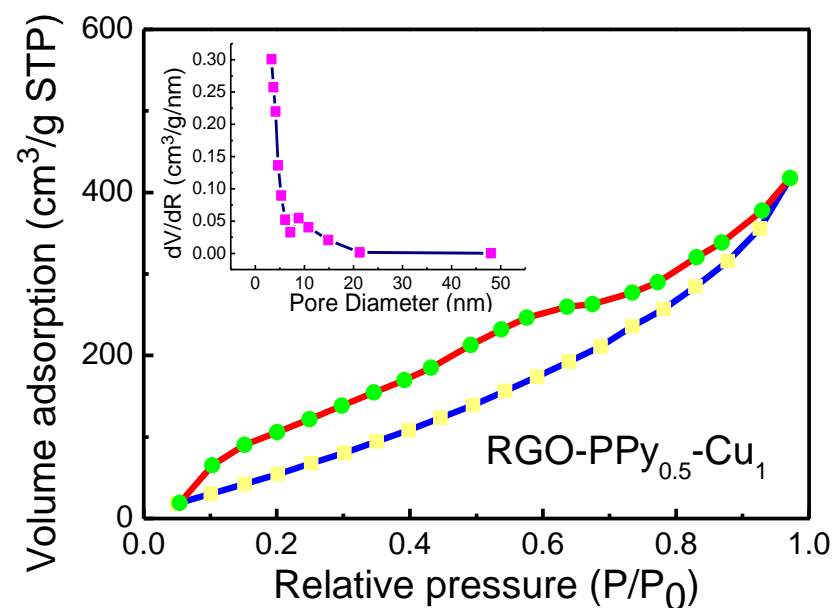


**Fig. S9** - Nitrogen sorption isotherm and pore size distribution (inset) of  $\text{RGO-PPy}_{0.5}\text{-Cu}_1$ .

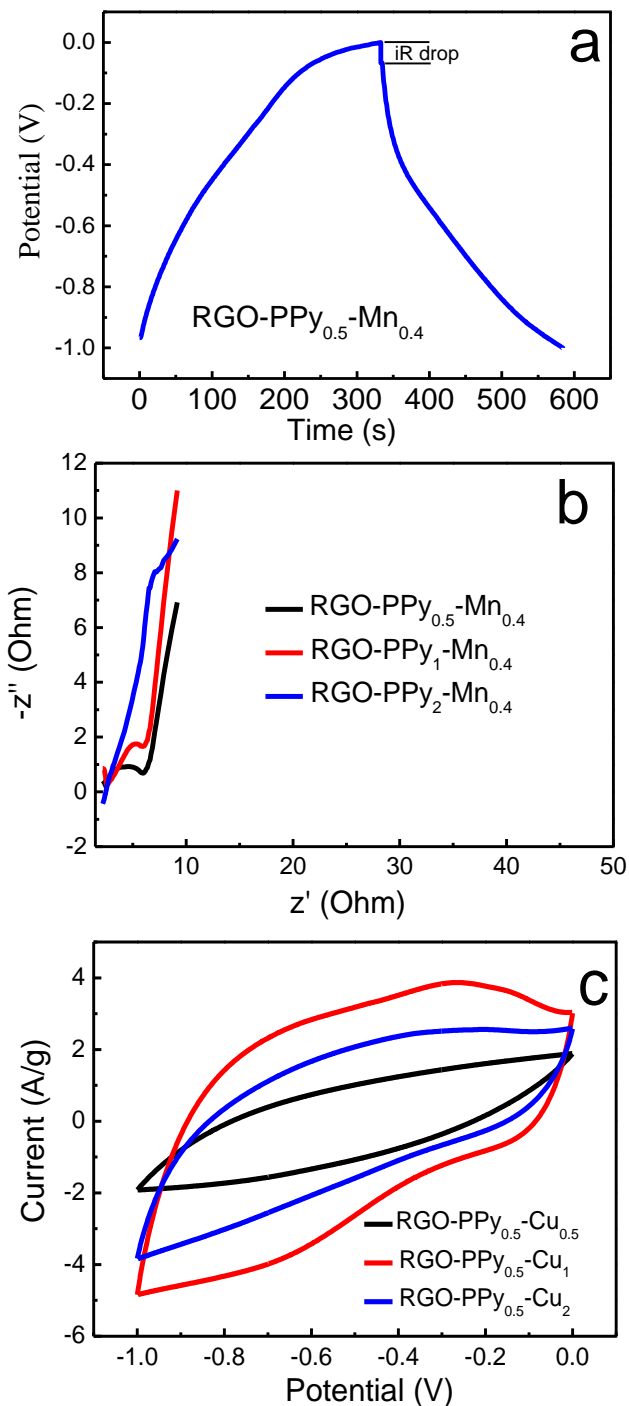


**Fig. S10** - (a) GC curves at a current of 1 A/g of RGO-PPy<sub>0.5</sub>-Mn<sub>0.4</sub> electrodes, iR drop was about 0.06 V. (b) Nyquist plots of the EIS for RGO-PPy-Mn electrodes and (c) CV curves of RGO-PPy-Cu electrodes at a scan rate of 10 mV/s.